Talanta 115 (2013) 381–385

Contents lists available at SciVerse ScienceDirect

Talanta

journal homepage: www.elsevier.com/locate/talanta

Detection of glutathione based on nickel hexacyanoferrate film modified Pt ultramicroelectrode by introducing cetyltrimethylammonium bromide and Au nanoparticles

Hongxia He [1], Jie Du [1], Yaqi Hu, Jing Ru, Xiaoquan Lu *

Key Laboratory of Bioelectrochemistry & Environmental analysis of Gansu Province, College of Chemistry & Chemical Engineering, Northwest Normal University, Lanzhou 730070, China

ARTICLE INFO

Article history:
Received 7 March 2013
Received in revised form
19 May 2013
Accepted 21 May 2013
Available online 3 June 2013

Keywords:
Glutathione
Nihcf/CTAB/AuNPs Pt UME
Electrochemical detection
Microsensor

ABSTRACT

A novel method for glutathione (GSH) detection in real blood sample with a nickel hexacyanoferrate (NiHCF) film modified Pt ultramicroelectrode (UME) was proposed. The electrochemical properties of NiHCF film modified Pt UME were improved by introducing cetyltrimethylammonium bromide (CTAB) and Au nanoparticles (AuNPs) into NiHCF film. The novel hybrid films (NiHCF/CTAB/AuNPs) were prepared by electrodepositing NiHCF and AuNPs in the presence of CTAB on the surface of Pt UME. The results indicated that the prepared NiHCF/CTAB/AuNPs Pt UME had a sensitive respond toward the oxidation of GSH and could be used for its selective determination in the presence of other coexisting interferents in real blood samples. The calibration curve for GSH was found to be linear from 0.2–1 μM, and the limit of detection ($S/N=3$) was 0.08 μM. The strategy explored here might provide a new pathway to design NiHCF/CTAB/AuNPs film microsensor for in situ detecting GSH, which had unique characteristics and potential applications in the fields of sensor and medical diagnosis.

1. Introduction

Glutathione has one primary amine, two amide groups, two carboxylic groups and one thiol group, which exists in a reduced form (GSH) and a oxidized form as glutathione disulfide (GSSG) [1]. The level of GSH is pivotal for biological functions in the organisms such as protein and DNA synthesis [2], enzyme activity [3], metabolism and cell protection [4]. It is an essential endogenous antioxidant that plays a critical part in cellular defense against toxins and free radicals [5].

A number of detection methods for GSH have been described in the literature in vitro studies, such as, CdS:Mn/ZnS core/shell quantum dots as fluorescent probes [6], high-performance liquid chromatography (HPLC) [7,8], spectrophotometry [9], chemiluminescence [10–12] and colorimetric assay [13]. However, these methods are complex, need time-consuming sample preparation, costly equipment and trained person to manipulate. Most importantly, they are unsuitable for intracellular GSH detection. Recently, electrochemical methods have been paid considerable attention due to their simplicity, rapidity, high sensitivity and low cost. In general, electrochemical sensors mostly based on oxidation of GSH on unmodified [14] or chemically modified electrodes [15–19]. They serve as part of a continuing interest in developing electrochemical sensors. Especially, NiHCF [20] could be regarded as an active cation-exchange matrix [21] since both oxidized and reduced NiHCF structures permit unimpeded transport of electrolyte cations of different sizes while providing charge balance during the system's redox reaction. Furthermore, UME has some unique features such as enhanced mass-transport rates, reduced double-layer capacitance, and less susceptibility to ohmic losses [22]. Thus, UMEs have been increasingly important for applications in bioanalysis [23,24].

This work was to demonstrate an amperometric inhibitor microbiosensor based on the NiHCF/CTAB/AuNPs Pt UME for the low level determination of GSH in real blood samples. A kind of NiHCF film modified Pt UME was prepared by electrodeposition and was used as a microsensor for GSH. The proposed NiHCF/CTAB/AuNPs Pt UME exhibited a high sensitivity, low detection limit, and high selectivity for GSH. Then, the microsensor could give in situ information on the concentration of GSH in blood samples, which had unique characteristics and potential applications in the fields of sensor and medical diagnosis.

2. Experimental

2.1. Chemicals and reagents

γ-L-glutamyl-L-cysteinyl-glycine (GSH) was purchased from Shanghai source leaves biological technology Co. Ltd. (Shanghai, China). Pt microwires with a diameter of 25 μm (99.95%, hard)

* Corresponding author. Tel.: +86 931 7971276; fax: +86 931 7971323.
E-mail address: luxq@nwnu.edu.cn (X. Lu).
[1] These authors contributed equally.

0039-9140/$ - see front matter © 2013 Elsevier B.V. All rights reserved.
http://dx.doi.org/10.1016/j.talanta.2013.05.054

were obtained from Shanghai Chenhua Instrument Limited Company (Shanghai, China). Borosilicate glasses (o.d. 1.0 mm, i.d. 0.58 mm) were purchased from Sutter Instrument Co. Alumina polishing powders with different particle sizes of 0.3 and 0.05 μm were purchased from Buehler. All other chemicals used in this study were analytical grade or higher and used as received without further purification. The phosphate buffer solution (PBS) was prepared using 0.02 M KH_2PO_4, 0.02 M K_2HPO_4 and 0.1 M KCl. Solutions were prepared with doubly distilled water and deoxygenated by purging with prepurified nitrogen gas. All experiments were performed at normal temperature.

2.2. Apparatus

A CHI 660 setup (CHI instrument, Co. Ltd., Austin, USA) was employed to perform cyclic voltammetry (CV) and differential pulse voltammetry (DPV) experiments by a three-electrode system consisting of modified Pt UME as a working electrode, a saturated calomel electrode (SCE) and a platinum electrode were used as reference electrode and counter electrode, respectively. A Sartorius basic pH meter PB-10 was purchased RenHe Instrument Co. Ltd. (Shanghai, China). A microelectrode puller was obtained Chengdu Instrument (WD-1, Sichuan, China).

2.3. Preparation and modification of Pt UMEs

Pt UMEs were constructed from 25 μm diameter Pt wire sealed in borosilicate glasses. The sealed end was removed with a diamond-coated cutting wheel to expose Pt microdisk. A Pt UME surface was polished lightly with 0.30 and 0.05 μm alumina slurry on the chamois, then it was rinsed thoroughly with doubly distilled water, and finally it was ultrasonicated in ethanol and deionized water for 5 min. Electrodeposition was performed using solutions containing 1.0 mM $K_3Fe(CN)_6$, 1.0 mM $HAuCl_4$, 1.0 mM Ni $(NO_3)_2$ and 2.0 mM CTAB and the procedure involved 40 voltammetric cycles at 50 mV s^{-1} in a potential range from 0 to 1.0 V. After deposition, the modified UME was rinsed with doubly distilled water and heated at 40 °C for 20 min.

3. Results and discussion

3.1. Electrochemical behavior and the formation mechanism of NiHCF/CTAB/AuNPs film

Steady growth of the NiHCF film (on the electrode surface) during repetitive potential cycling solution (as described in Section 2) was clearly apparent from both the peak current increase in cyclic voltammetry (Fig. 1). As shown in Scheme 1, $AuCl_4^-$ was reduced (Eq. (1)) and deposited on the electrode surface [25,26]. Alternatively, CTAB could be assembled on the AuNPs and assisted Fe^{3+}/Ni^{2+} absorption. The presence of CTAB in solution could also assist NiHCF deposition on the UME surface during film formation [27,28], which suggested that CTAB was adsorbed to hydrophilic ionic groups on the surface of the electrode through its polar head groups [28]. The NiHCF/CTAB/AuNPs film was generated during reduction cycles, i.e. upon reduction of $[Fe^{III}(CN)_6]^{3-}$ to $[Fe^{II}(CN)_6]^{4-}$ [29]. While appearance of the voltammetric peaks at more positive potentials (0.6 V) is indicative of the formation of K^+ rich structures in which the ratio of Ni to Fe is close to 1, the growth of peaks at about 0.47 V reflects the generation of Ni^{2+} rich structures in which ratio of Ni to Fe is close to 1.5. The reactions possibly occur as follows Eqs. 3, 4. Therefore, two pairs of redox peaks are clearly displayed in formation of NiHCF [30,31]. Possible

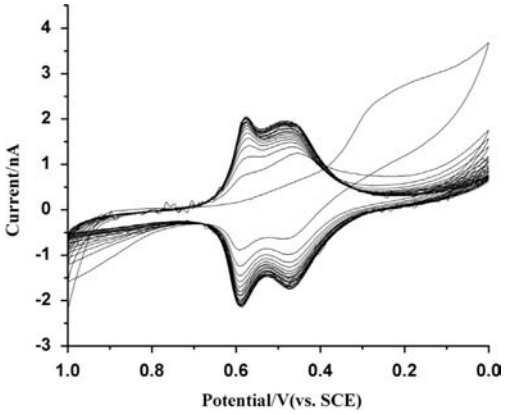

Fig. 1. CVs of NiHCF/CTAB/AuNPs Pt UME recorded in 1.0 mM $K_3Fe(CN)_6$, 1.0 mM $HAuCl_4$, 1.0 mM $Ni(NO_3)_2$ and 2 mM CTAB solution. Scan rate: 50 mV s^{-1}.

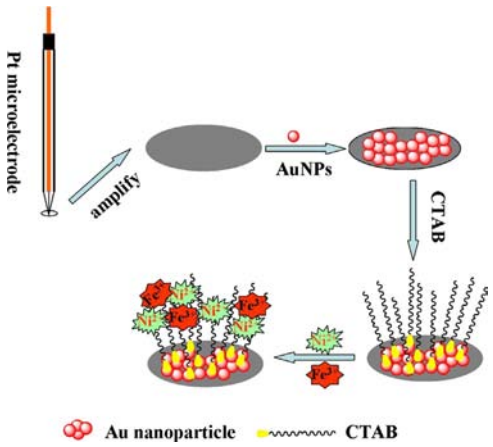

Scheme 1. Preparation of GSH microbiosensor based on NiHCF/CTAB/AuNPs Pt UME.

mechanisms of NiHCF/CTAB/AuNPs films were stated as following:

$$AuCl_4^- + 3e^- \rightarrow Au(0) + Cl^- \quad (1)$$

$$[Fe(CN)_6]^{3-} + 3e^- \rightarrow [Fe(CN)_6]^{4-} \quad (2)$$

$$[Fe(CN)_6]^{4-} + Ni^{2+} + 2K^+ \rightarrow K_2Ni[Fe(CN)_6] \quad (3)$$

$$[Fe(CN)_6]^{4-} + 1.5Ni^{2+} + K^+ \rightarrow KNi_{1.5}[Fe(CN)_6] \quad (4)$$

3.2. Characterization of NiHCF/CTAB/AuNPs Pt UME

Morphology of Pt UME was characterized by SEM. Fig. 2A shows a SEM image of a relatively large Pt UME which radius is about to 25 μm. Fig. 2B is a SEM image of a Pt UME after being deposited the NiHCF/CTAB/AuNPs film. As it can be seen, the smooth NiHCF/CTAB/AuNPs film without cracks is observed on the Pt UME surface (Fig. 2B).

3.3. Characterization of electrochemical behavior of NiHCF/CTAB/AuNPs Pt UME

The CVs of 1 μM GSH on both the bare UMEs and the NiHCF/CTAB/AuNPs Pt UME are shown in Fig. 3. No redox peaks can be observed on the bare UMEs with or without GSH (Fig. 3a, b), while two couple of well-defined, reversible redox peaks appear on the electropolymerized NiHCF/CTAB/AuNPs film Pt UME in the presence and absence of GSH (Fig. 3c, d). It shows that the NiHCF film is successfully constructed [30,31]. The current signal obtained on

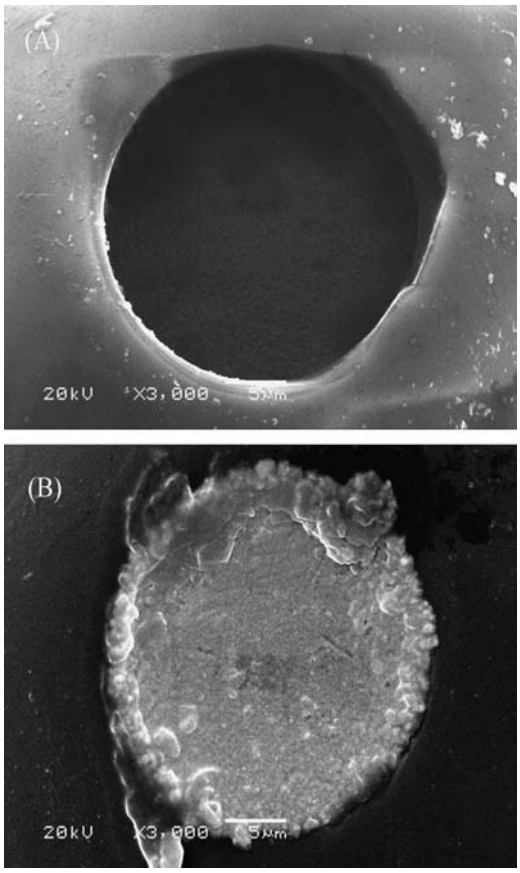

Fig. 2. The SEM images of (a) Pt UME, (b) Pt UME after being deposited NiHCF/CTAB/AuNPs film.

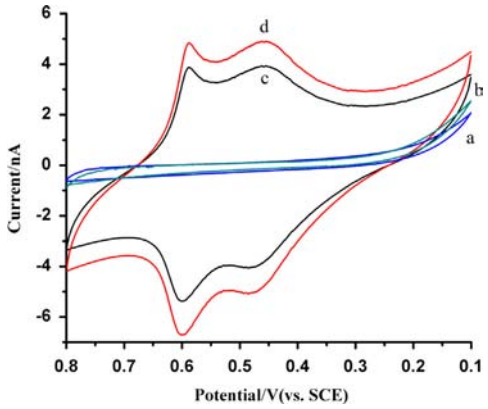

Fig. 3. CVs of the bare and NiHCF/CTAB/AuNPs modified Pt UME in the presence (a, c) or absence (b, d) of 1 μM GSH in 0.02 M PBS (pH=6.5). Scan rate: 50 mV s^{-1}.

the NiHCF/CTAB/AuNPs Pt UME in the absence of GSH is stronger than that in the presence of GSH. It possibly can be attributed to competitive oxidation between NiHCF and GSH.

3.4. Effect of pH on the electrochemical behavior of GSH

The effect of pH value on the electrochemical behavior of 1 μM GSH at NiHCF/CTAB/AuNPs Pt UME was carefully investigated by DPVs for wider range of pH from 3.0 to 9.0. From Fig. S1A, B (Supporting Information), it can be seen that the current response of GSH gradually increase as pH increasing from 3 to 6.5 and decrease with a further increase in pH up to 9.0 at 0.6 V and 0.47 V. So it displays that GSH biosensor exhibits the best current response in the solution of pH 6.5. When pH is between 3.0 and 6.5, $Fe(CN)_6^{3-}$ will be protonated [32]. When pH increase from 7.0 to 9.0, the cause for this action may be attributed to the strong interaction between ferric ions and hydroxyl ions (OH^-) which forms $Fe(OH)_3$ at higher pH [33], resulting in the destruction of the Fe–CN–Ni bond, so it leads to NiHCF film is not stable.

3.5. Effect of scan rates on the electrochemical behavior of GSH

Fig. S2(Supporting Information) shows CVs of 1 μM GSH in 0.02 M PBS with different scan rates from 2 to 70 mV s^{-1}. The redox peak currents increase with scan rates increasing. Each of CV curves exhibits two couple of well-defined, reversible redox with peaks at 0.59/0.6 V and 0.45/0.47 V. A pair linear relationship can be obtained for the redox peak potential at 0.59/0.6 V (Fig. S2A). The regression equations can be expressed as I_{pc}=0.076 V+0.068 (nA, mV s^{-1}, R=0.9930) and I_{pa}=−0.097 V −0.635 (nA, mV s^{-1}, R=0.9923). Fig. S2B also indicates the relationships between the peak current (I_p) and scan rates (V). The regression equations for the redox peak potential at 0.45/0.47 V can be expressed as I_{pc}=0.072 V+0.387 (nA, mV s^{-1}, R=0.9916) and I_{pa}=−0.075 V −0.446 (nA, mV s^{-1}, R=0.9922), which strongly suggests that the redox reactions of GSH are adsorp-controlled.

3.6. Calibration curve

The DPVs signal on NiHCF/CTAB/AuNPs Pt UME for a series of samples with varying glutathione concentrations (0.2–8.0 μM) were investigated under the optimal experimental conditions. The resultant DPVs were then recorded and shown in Fig. 4. The peak currents decreased with increasing concentration of GSH. The calibration curves between the oxidation peak current (I_p) and the GSH concentration (c) are depicted in Fig. 4B, C. The curve is consisted by two sections, and which can be described by the regression equation I_{pa}=0.42c–8.98 (r=0.9913), I_{pa}=0.25c–7.19 (r=0.9987) at 0.58 V and 0.45 V, respectively, at the 0.2 to 1 μmol GSH concentration linear range.

3.7. Interferences

A systematic study was carried out under optimal experimental conditions to evaluate the interferences of the NiHCF/CTAB/AuNPs Pt UME for foreign substances on the detection of GSH. It was well known that ascorbic acid (AA), epinephrine (Ep), and dopamine Hydrochloride (DA. HCl) can coexist along with GSH in real samples like blood and physiological fluids. The peak currents can be measured by DPV whatever in the absence or presence of foreign species. It was demonstrated the oxidation signal could not be interfered with common interferents. The change values of peak current of GSH were listed in Table 1 (signal change below 10%).

3.8. Reproducibility and stability

To investigate the precision of the determination, six different electrodes constructed by the same procedure were analyzed. The relative standard deviation (RSD) of the current responses was 3.0%. The same NiHCF/CTAB/AuNPs Pt UME has been stored in the refrigerator for 7 days, it retained 99.3% of its initial current. The stability of the modified electrode was further confirmed by using the same electrode for repetitive measurement in a solution containing GSH. The relative standard deviation in the peak current was calculated to be 1.5%. Hence, it is obvious that the proposed NiHCF/CTAB/AuNPs Pt UME shows excellent stability and reproducibility.

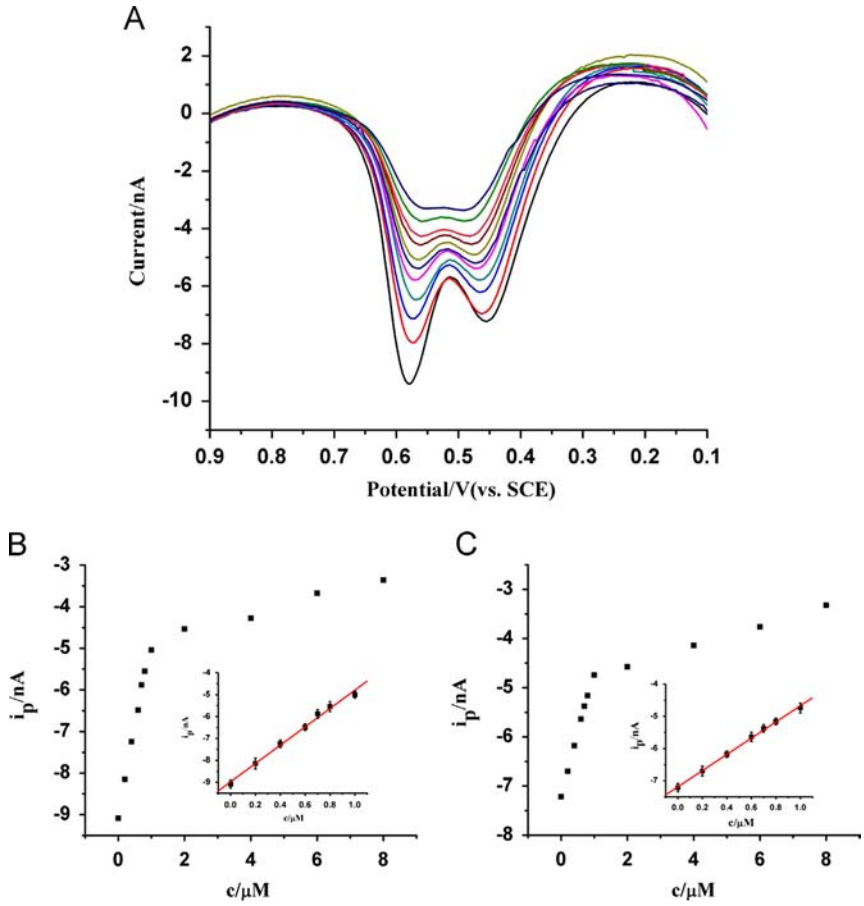

Fig. 4. (A) DPVs of different concentrations of GSH (0.2–8.0 μM) at NiHCF/CTAB/AuNPs Pt UME. (B and C) Relationships between the concentration of GSH and current response. The inset was calibration curve. Error bars represent the standard deviation for three independent measurements.

Table 1
The current changes from add different distractors.

	AA		DA. HCl		Ep	
Peak potential (V)	0.43	0.57	0.43	0.57	0.43	0.57
The current before add distractors (nA)	−4.67	−4.37	−4.67	−4.37	−4.67	−4.37
The current after add distractors (nA)	−4.41	−3.94	−4.58	−4.27	−4.4	−4.32
Current change value (%)	5.57	9.84	1.93	2.29	5.78	1.14

4. Conclusions

We successfully prepared microsensor based on Pt UME modified with NiHCF/CTAB/AuNPs to detect GSH in human blood sample. It was readily prepared by introducing CTAB and Au nanoparticles at pH 6.5, which performed high electrocatalytic activity and stability for the oxidation of GSH. It provides a promising way for the situ monitoring of GSH in human blood sample. Hence, the proposed NiHCF/CTAB/AuNPs Pt UME has great potential applications in the fields of sensor and medical diagnosis.

Acknowledgments

This work was supported by the National Natural Science Foundation of China (Nos. 21175108 and 21165015), the Science and Technology Support Projects of Gansu Province (No. 1011GKCA025). The author also would like to gratefully acknowledge all the members for the assistance of this work.

Appendix A. Supporting information

Supplementary data associated with this article can be found in the online version at http://dx.doi.org/10.1016/j.talanta.2013.05.054.

References

[1] N. Kaplowitz, T.Y. Aw, M. Ookhtens, Ann. Rev. Pharmacol. Toxicol 25 (1985) 714–744.
[2] M. Gunaratnam, M.H. Grant, Toxicol. in Vitro 22 (2008) 879–886.
[3] M. Raffa, A. Mechri, L.B. Othman, C. Fendri, L. Gaha, A. Kerkeni, Prog. Neuro-Psychoph 33 (2009) 1178–1183.
[4] Y. Wang, M. Qiao, J.J. Mieyal, L.M. Asmis, R. Asmis, Free Radical Bio. Med 41 (2006) 775–785.
[5] S.C. Lu, Mol. Aspects Med 30 (2009) 42–59.
[6] S. Banerjee, S. Kar, J.M. Perez, S. Santra, J. Phys. Chem. C 113 (2009) 9659–9663.
[7] M.L. Steele, L. Ooi, G. Münch, Anal. Biochem. 429 (2012) 45–52.
[8] A.K. Sakhi, R. Blomhoff, T.E. Gundersen, J. Chromatogr. A 1142 (2007) 178–184.
[9] M. Catal 'a, I. cardo, L. Lahuerta Zamora, J. Mart'ınez Calatayud, Analyst 123 (1998) 1685–1689.
[10] A.A. Ensafi, T. Khayamian, F. Hasanpour, J. Pharmaceut., Biomed 48 (2008) 140–144.

[11] C. Lu, Q. Li, S. Chen, L. Zhao, Z. Zheng, Talanta 85 (2011) 476–481.
[12] S. Wang, H. Ma, J. Li, X. Chen, Z. Bao, S. Sun, Talanta 70 (2006) 518–521.
[13] N. Uehara, K. Ookubo, T. Shimizu, Langmuir 26 (2010) 6818–6825.
[14] W. Jin, X. Zhao, L. Xiao, Electroanal 12 (2000) 858–862.
[15] S.Y. Chee, M. Flegel, M. Pumera, Electrochem. Commun 13 (2011) 963–965.
[16] P. Miao, L. Liu, Y. Nie, G. Li, Biosens. Bioelectron 24 (2009) 3347–3351.
[17] J. Narang, N. Chauhan, P. Jain, C.S. Pundir, Int. J. Biol. Macromol 50 (2012) 672–678.
[18] P. Muthirulan, R. Velmurugan, Colloid. Surface B 83 (2011) 347–354.
[19] A. Ambrosi, M. Pumera, Chem. Eur. J 16 (2010) 1786–1792.
[20] P.C. Pandey, A.K. Pandey, Analyst 137 (2012) 3306–3313.
[21] M.T. Kelly, G.A. Arbuckle-Keil, L.A. Johnson, E.Y. Su, L.J. Amos, J.K.M. Chun, A. B. Bocarsly, J. Electroanal. Chem. 500 (2001) 311–321.
[22] R.W. Murray, Chem. Rev 108 (2008) 2688–2720.
[23] P.S. Cahill, Q.D. Walker, J.M. Finnegan, G.E. Mickelson, E.R. Travis, R. M. Wightman, Anal. Chem 68 (1996) 3180–3186.
[24] F.J.M. Hoeben, F.S. Meijer, C. Dekker, S.P.J. Albracht, H.A. Heering, S.G. Lemay, ACS Nano 2 (2008) 2497–2504.
[25] J. Du, Y. Wang, X. Zhou, Z. Xue, X. Liu, K. Sun, X. Lu, J. Phys. Chem. C 114 (2010) 14786–14793.
[26] H. Yu, Q.-L. Sheng, L. Li, J.-B. Zheng, J. Electroanal. Chem. 606 (2007) 55–62.
[27] R. Vittal, K.-J. Kim, H. Gomathi, V. Yegnaraman, J. Phys. Chem. B 112 (2008) 1149–1156.
[28] S.M. Senthil Kumar, K.Chandrasekara Pillai, J. Electroanal. Chem 589 (2006) 167–175.
[29] J. Bácskai, K. Martinusz, E. Czirók, G. Inzelt, P.J. Kulesza, M.A. Malik, J. Electroanal. Chem 385 (1995) 241–248.
[30] S. Zamponi, M. Berrettoni, P.J. Kulesza, K. Miecznikowski, M.A. Malik, O. Makowski, R. Marassi, Electrochim. Acta 48 (2003) 4261–4269.
[31] O. Makowski, B. Kowalewska, D. Szymanska, J. Stroka, K. Miecznikowski, B. Palys, M.A. Malik, P.J. Kulesza, Electrochim. Acta 53 (2007) 1235–1243.
[32] S. Iijima, T. Ichihashi, Nature 363 (1993) 603–605.
[33] Z. Li, J. Chen, W. Li, K. Chen, L. Nie, S. Yao, J. Electroanal. Chem 603 (2007) 59–66.